Acta Materialia Turcica

Volume 4, June 2020, Pages 1-8

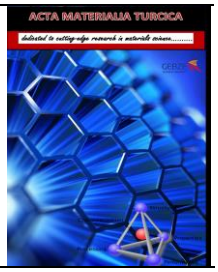

Application of Angle Diversity Technique to Optical Wireless Communication Systems for Smartphones

S. RYU

Meiji University, School of Interdisciplinary Mathematical Sciences
4-21-1, Nakano, Nakano-ku, Tokyo 164-8525, Japan

Abstract:

Much attention has been given to optical wireless communication (OWC) systems since the systems have a possibility to offer wideband communication channel, e.g., inside building environment. In this context, the application of the OWC technology to smartphone communication is of great interest. It is possible to construct the angle diversity receiving systems using multiple receivers on the surfaces of a smartphone device to achieve stable communication when a smartphone moves around two-dimensionally and rotates three-dimensionally. An angle diversity configuration with multiple receivers facing different directions have been reported. The literature is only focused on the condition when the receivers are supposed to move around two-dimensionally. But three-dimensional rotation of the device has not been well considered. In this paper, we consider the OWC systems for a smartphone that is supposed to move around two-dimensionally and rotate three-dimensionally. Computer simulation has been performed for the maximal-ratio combining of the output of four receivers placed on the top, front, right, and left surfaces of a smartphone device. It has been made clear that the diversity receiving systems using four receivers give stable signal-to-noise ratio performance under realistic usage condition of a smartphone. It has also been found that a semi-angle field-of-view of a receiver should be at least 60 degrees to achieve stable performance.

Keywords: Optical Wireless Communication; Visible Light Communication; Angle Diversity; Maximal-Ratio Combining ; Equal-Gain Combining

DOI:

1. INTRODUCTION

Much attention has been given to optical wireless communication (OWC) systems since the systems have a possibility to offer wideband communication channel, e.g., inside building environment [1,2]. In this context, the application of the OWC technology to smartphone communication is of great interest. It is possible to construct the angle diversity receiving systems using multiple receivers on the surfaces of a smartphone to achieve stable communication when a smartphone moves around and rotates three dimensionally. An angle diversity configuration with multiple receivers facing different directions have been reported [3-5]. But the literature is only focused on the condition when the receivers never rotate three dimensionally. In this paper, we consider the OWC systems for a smartphone that is supposed to rotate three dimensionally. Computer simulation has been performed for diversity combining of the output of four receivers placed on the top, front, right, and left surfaces of a smartphone. It has been made clear that the diversity receiving systems using the four receiver

Corresponding Author E-mail: sryu@meiji.ac.jp

Acta Materialia Turcica

Volume 4, June 2020, Pages 1-8

output give stable signal-to-noise ratio (SNR) performance under realistic usage condition of a smartphone.

2. SYSTEM MODEL

Figure 1 shows a system model used for computer simulation. A room with a width of 5 m and a depth of 5 m are assumed. On the four corners of a ceiling, optical transmitters (TX1, TX2, TX3, and TX4) are installed. All the transmitters are facing directly below. Three dimensional axes (x, y, and z) are assumed as shown in Figure. 1. A top surface of a smartphone is supposed to move on x-y plane, and the distance between the top surface of the smartphone and the ceiling is assumed to be 3 m. A smartphone is equipped with four receivers that are placed on top (RX1), right (RX2), left (RX3), and front (RX4) surfaces. We set x_0, y_0, and z_0 axes on the smartphone as shown in Figure. 1. The smartphone is assumed to rotate along each axis considering realistic usage condition. We define a 'roll' angle α along x_0 axis, a 'pitch' angle β along y_0 axis, and a 'yaw' angle γ along z_0 axis as shown in Figure. 1.

If we apply the OWC technology to a smartphone, a part of light from the transmitters enters a receiver over a human head, i.e., a part of a front surface of a smartphone is usually shaded by it. Figure. 2 shows such a situation. In the simulation, it is assumed that a human head is a sphere with a diameter of 0.3 m, and that the distance between RX4 and the head sphere is 0.2 m. Hence, the light within a cone in Figure 2 is blocked by the human head. The angle ϕ_a in Figure 2 can be calculated to be 25.4°. We used these values throughout the simulation.

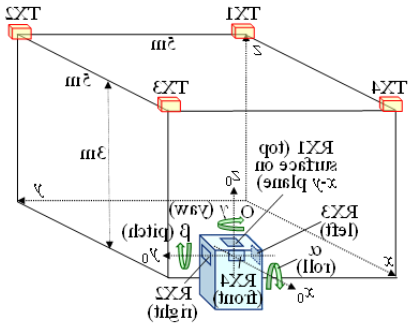

Figure 1. System model.

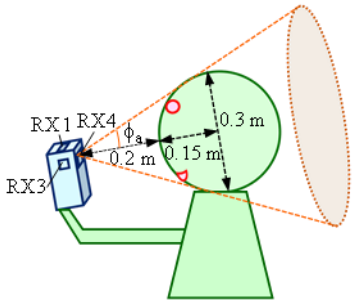

Figure 2. Shading of front surface of smartphone by human head.

3. FUNDAMENTAL THEORY

In the OWC system using an LED as a transmitter, the dc channel gain, G, is generally shown as [1,2]

$$G = \begin{cases} \dfrac{(m+1)A}{2\pi h^2}\cos^m \varphi_T T_s(\varphi_R) g(\varphi_R)\cos\varphi_R & (\varphi_R \le \varphi_C) \\ 0 & (\varphi_R > \varphi_C) \end{cases} \quad (3.1)$$

where h is the distance between a transmitter and a receiver, A is physical area of a photodetector, ϕT is the angle of irradiance, m is the order of Lambertian radiation and determined by the semi-angle of half illuminance of an LED ($\theta_{1/2}$), i.e,, $m = -\ln 2 / \ln(\cos\theta_{1/2})$, ϕ_R is the angle of incidence, ϕ_C is a field of view (FOV) of a receiver , Ts(ϕR) is the signal transmission of a filter, g(ϕR) is the concentrator gain. Optical power at each receiver input can be calculated using (1). In the simulation, intensity-modulation direct-detection (IM-DD) on-off keying system with binary non-return-to-zero (NRZ) data stream is assumed.

In the model described above, as shown in Figure 3, four output signals of the receivers can be combined according to diversity combining techniques [6]. In Figure 3, si(t) (i=1, 2, 3, 4) is the output signal current of a receiver i when the signal is in the 'mark' (on) state, wi is the weighting factor for si(t). Then, total output current of a combining circuit, r(t), can be obtained as

$$r(t) = \sum_{i=1}^{4} w_i \{ s_i(t) + n_i(t) \} \quad (3.2)$$

where ni(t) is the output noise current at a receiver i. In the system if we use a pin photodiode, the shot noise due

Corresponding Author E-mail: sryu@meiji.ac.jp

Acta Materialia Turcica

Volume 4, June 2020, Pages 1-8

to the input light to each receiver is considered to be small as compared with the thermal noise of the receiver, so the noise power at the output of the receiver is dominated by receiver thermal noise Hence, the noise power of each receiver, N_0, can be assumed to be the same, i.e.,

$$N_0 \equiv \overline{n_i^2(t)} \text{ for all } i \tag{3.3}$$

where $\overline{n_i^2(t)}$ is the ensemble average of $n_i^2(t)$. Hence, the SNR of r(t), $\Gamma(t)$, can be obtained as

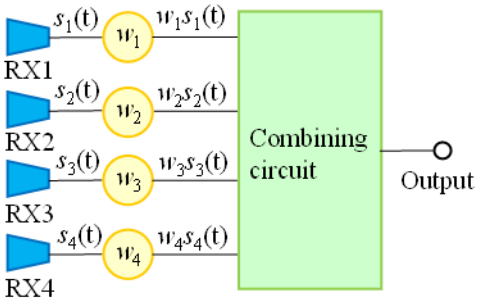

Figure 3. Diversity receiving system.

$$\Gamma(t) = \frac{\left(\sum_{i=1}^{4} w_i s_i(t)\right)^2}{\left(\sum_{i=1}^{4} w_i n_i(t)\right)^2} = \frac{\left(\sum_{i=1}^{4} w_i s_i(t)\right)^2}{\sum_{i=1}^{4} w_i^2 \cdot N_0}. \tag{3.4}$$

In deriving (4), we assumed that the noise in each receiver is independent statistical process. If we apply Schwarz inequality to (4),

$$\Gamma(t) = \frac{\left(\sum_{i=1}^{4} w_i s_i(t)\right)^2}{\sum_{i=1}^{4} w_i^2 \cdot N_0} \le \frac{\sum_{i=1}^{4} w_i^2 \sum_{i=1}^{4} s_i^2(t)}{\sum_{i=1}^{4} w_i^2 \cdot N_0} = \frac{\sum_{i=1}^{4} s_i^2(t)}{N_0}. \tag{3.5}$$

Equality in (5) holds when w_1: w_2: w_3: w_4= $s_1(t)$: $s_2(t)$: $s_3(t)$: $s_4(t)$. If we suppose the received optical power at a receiver i at time t as $P_i(t)$, $s_i(t)$ can be calculated as

$$s_i(t) = RP_i(t) \tag{3.6}$$

where R is the responsivity of an photodetector in an optical receiver that is assumed to be the same for all the receives. Using (6) in (5) yields

$$\Gamma(t) = \frac{R^2\left(\sum_{i=1}^{4} w_i P_i(t)\right)^2}{\sum_{i=1}^{4} w_i^2 \cdot N_0} \le \frac{R^2 \sum_{i=1}^{4} P_i^2(t)}{N_0}. \tag{3.7}$$

As for diversity receiving systems, we can consider the equal-gain combining (EGC) and maximal-ratio combining (MRC) methods. In the MRC technique, the weighting factor for each signal is set to be proportional to the signal level, i.e., w_1: w_2: w_3: w_4= $s_1(t)$: $s_2(t)$: $s_3(t)$: $s_4(t)$, so that equality in (7) holds. Hence, the achieved SNR for the MRC method, $\Gamma_{MRC}(t)$, is shown as

$$\Gamma_{MRC}(t) = \frac{R^2 \sum_{i=1}^{4} P_i^2(t)}{N_0} \tag{3.8}$$

that is the summation of the SNR of each receiver. For the EGC method, each receiver output is simply added, so the weighting factor is set to be 1 for every receiver, the achieved SNR, $\Gamma_{EGC}(t)$ is calculated as

$$\Gamma_{EGC}(t) = \frac{R^2\left(\sum_{i=1}^{4} P_i(t)\right)^2}{4N_0} \tag{3.9}$$

4. PERFORMANCE OF ANGLE DIVERSITY RECEIVING TECHNIQUE

In the simulation in this paper, the SNR has been evaluated against the reference SNR value when a smartphone is placed at coordinates (0,0,0) with upright position (α=β=γ=0) and only RX1 was in operation. The obtained SNR values are called 'relative SNR' in this paper. It was also assumed that $\theta_{1/2}$=30° for all the transmitters. In the simulation an FOV (semi-angle) of the receiver was assumed to be 60°.

Figure 4 shows relative SNR distribution when RX1 and RX4 are in operation in case of the MRC and EGC methods when α=β=γ= 0°. We can see from Figure 4 that

Corresponding Author E-mail: sryu@meiji.ac.jp

Acta Materialia Turcica

Volume 4, June 2020, Pages 1-8

the MRC performs better than the EGC as is predicted from the theory in Chapter 3, so we will perform the simulation only for the MRC method in the following discussion

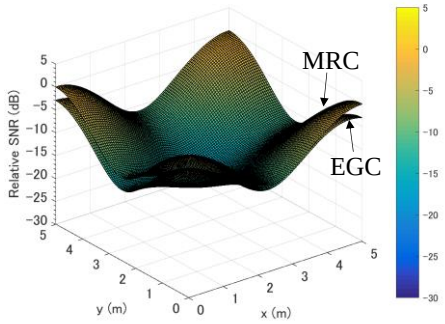

Figure 4. Relative SNR when α=β=γ=0° for MRC and EGC (RX1+RX4).

Figures 5(a)~(f) show relative SNR distribution for a single receiver and multiple receiver configuration with an MRC technique when a smartphone moves on *x*-*y* plane for α=γ=0° and β=-30° without shading by human head. It can be seen from Figures. 5(a)~(f) that the MRC technique for RX1+RX4 and RX1+RX2+RX3+RX4 give improved SNR characteristics as compared with the single receiver configuration.

Figure 6(a)~(f) show relative SNR distribution for the same assumptions as in Figures 5 when a part of the front surface of a smartphone is shaded by a human head as shown in Figure. 2. If we compare Figure 5(b) and Figures 6(b), we can see that the SNR distribution for RX4 only case is strongly affected by a human head. The reason for this is that RX4 is the most severely shaded by a human head as is shown in Figure 2. However, even in such a condition, we see little SNR degradation by applying the MRC technique to RX1+RX4 and RX1+RX2+RX3+RX4 configuration. From the results, we can say that the angle diversity technique is effective even if a part of the surface of a smartphone is shaded by a human head.

Next, we considered more realistic conditions when α=30°, β=-30°, and γ= 45°. Figures. 7(a)~(f) show relative SNR distribution examples for a single receiver and multiple receiver configuration. From Figures 7(a)-(b), (c), and (d), we can see that only a single receiver will not provide stable performance when roll, pitch, and yaw angles vary. From Figure 7(e), it is seen that two-receiver configuration on the top and front surfaces provide better performance as compared with a single receiver configuration, but this configuration lacks tolerance for roll angle variation. The best performance is provided when all the receivers are used under diversity combining as shown in Figure 7(f).

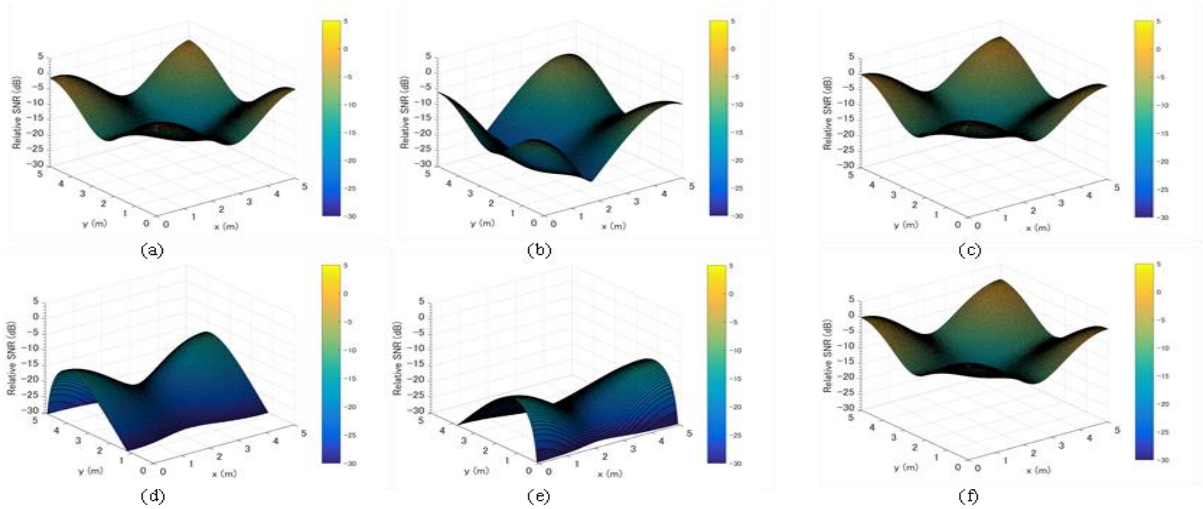

Figure 5. Relative SNR distribution when α=γ=0° and β=30° for various receiver configurations without shading by human head; **a.** RX1 only, **b.** RX4 only, **c.** RX1+RX4, **d.** RX2 only, **e.** RX3 only, and **f.** RX1+RX2+RX3+RX4.

Corresponding Author E-mail: sryu@meiji.ac.jp

Acta Materialia Turcica

Volume 4, June 2020, Pages 1-8

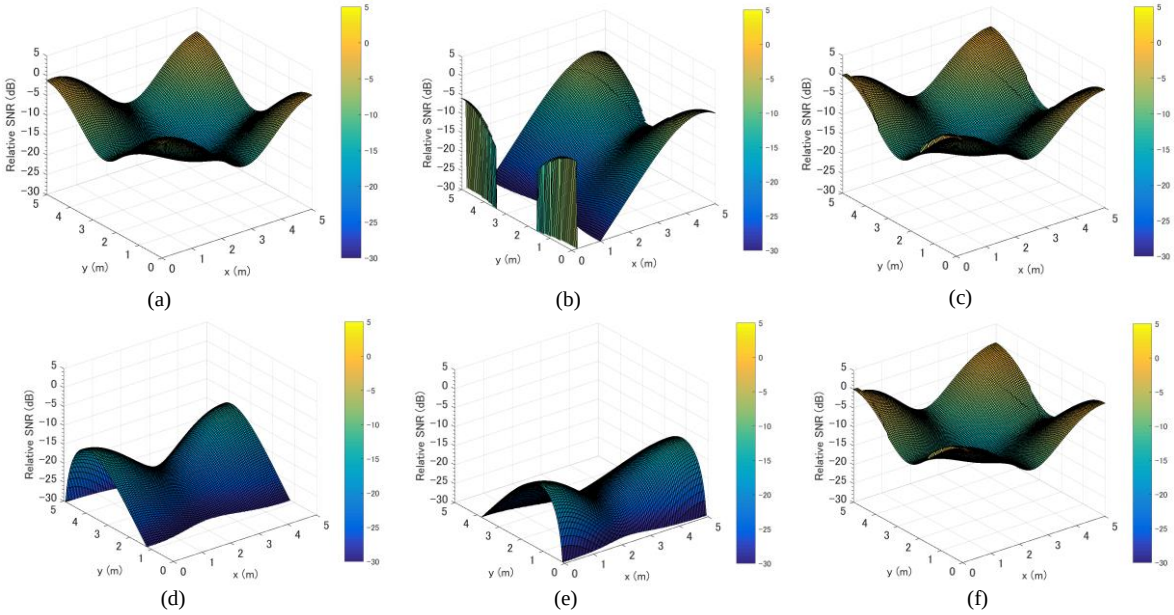

Figure 6. Relative SNR distribution when α=γ=0° and β=-30° for various receiver configurations with shading by human head; **a.** RX1 only, **b.** RX4 only, **c.** RX1+RX4, **d.** RX2 only, **e.** RX3 only, and **f.** RX1+RX2+RX3+RX4.

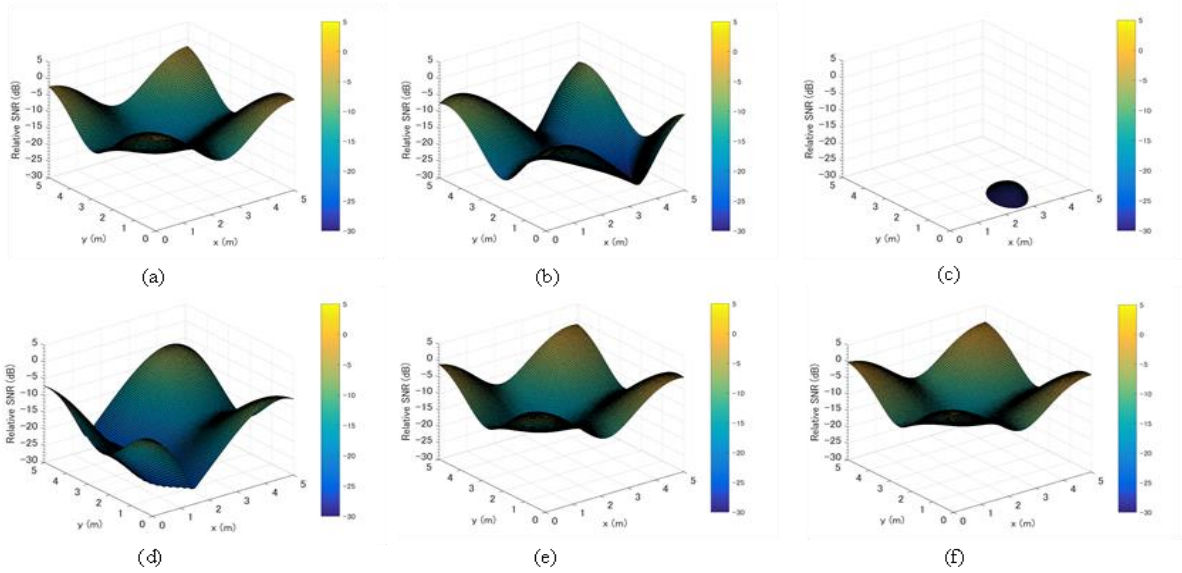

Figure 7. Relative SNR distribution when α=30°, β=-30°, and γ=45° for various receiver configurations; **a.** RX1 only, **b.** RX2 only, **c.** RX3 only, **d.** RX4 only, **e.** RX1+RX4, and **f.** RX1+RX2+RX3+RX4.

Corresponding Author E-mail: sryu@meiji.ac.jp

Acta Materialia Turcica

Volume 4, June 2020, Pages 1-8

To examine the above results more in details, simulation was performed when only RX1 was used. Figure 8 shows the results. In Figure 8(a), roll angle (α) was varied from 0° to 90° when β=-30° and γ=45°. In Figure. 8(a), relative SNR was calculated over the whole x-y plane for each α, and the maximum and minimum SNR over the x-y plane was plotted. As is seen from Figure 8(a), the SNR is degraded as α is increased. Similar tendency is observed in Figure 8 (b) in which β is changed when α=30 ° and γ=45 °. Figure 8 (c) shows the results when γ is changed. The curve is almost flat since the smartphone is just rotated around z_0-axis, but the maximum SNR is degraded by about 2 dB compared with the reference SNR. Similar simulation was carried out when all the receivers are used under the MRC configuration and the results are shown in Figure 9. We can see that all the results show almost flat SNR for the change of α, β, and γ, and the maximum SNR is almost recovered to the reference SNR, which shows the effectiveness of an angle diversity receiver configuration with four receivers.

5. PARAMETERS INFLUENDING SYSTEM PERFORMANCE

In Chapter IV, we have made clear that an angle diversity receiver configuration proposed in this paper can achieve stable SNR when a smartphone moves in a realistic usage condition. In this Chapter, we also consider the influence of the following parameters on the system performance, i.e., a semi-angle of half illuminance of an LED and an FOV of a receiver.

First, the influence of a semi-angle of half illuminance of an LED ($\theta_{1/2}$) was examined. Figures. 10(a), (b), and (c) show the minimum relative SNR versus $\theta_{1/2}$ when α, β, or γ is hanged by 90°. Other parameters assumed are shown in figure captions. From Figures 10, we can see that the optimum value of $\theta_{1/2}$ is about 55 ° for all the cases. Hence, we can say that it is necessary to use an LED with a $\theta 1_{/2}$ of about 55° to achieve the optimum SNR.

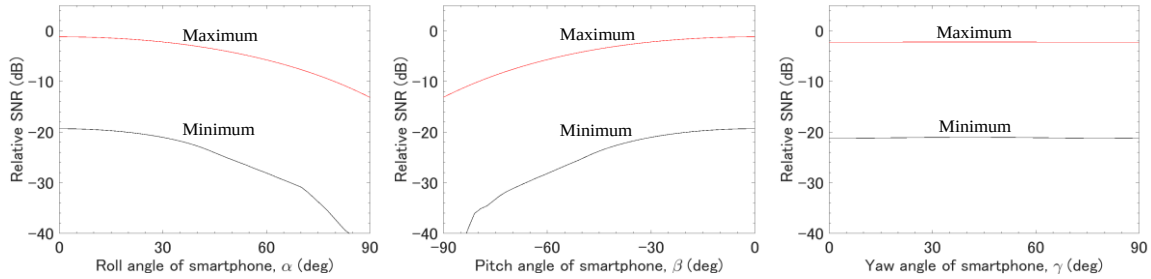

Figure 8. Relative SNR when α, β, or γ is varied with only RX1 used; **a.** β=-30° and γ=45°, **b.** α=30° and γ=45°, and **c.** α=30° and β=-30°.

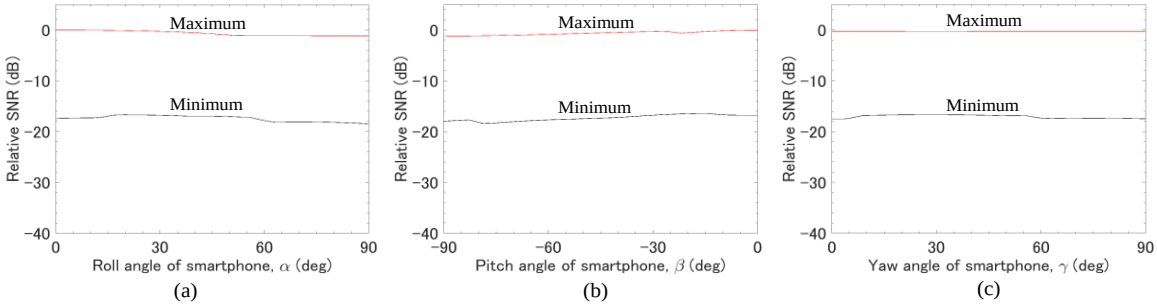

Figure 9. Relative SNR when α, β, or γ is varied with all the receivers (RX1~RX4) used; **a.** β=30° and γ=45°, **b.** α=30° and γ=45°, and **c.** α=30° and β=30° .

Corresponding Author E-mail: sryu@meiji.ac.jp

Acta Materialia Turcica

Volume 4, June 2020, Pages 1-8

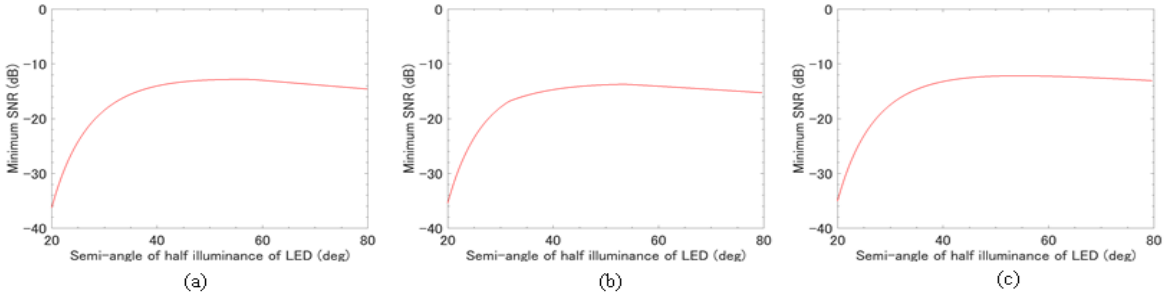

Figure 10. Minimum relative SNR versus $\theta_{1/2}$ when α, β, or γ is varied with all the receivers (RX1~RX4) used; **a.** 0°≤α≤90°,β=-30°, and γ=45°, **b.** α=30°, -90°≤β≤0°, and γ=45°, and **c.** α=30°, β=-30°, and 0°≤γ≤90°.

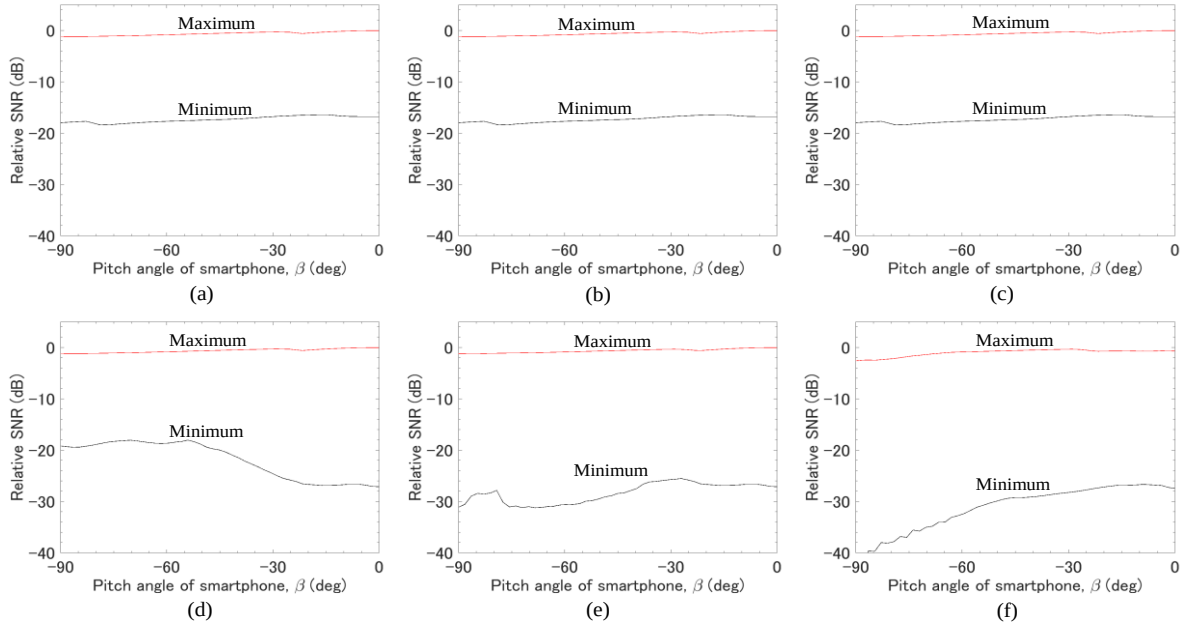

Figure 11. Relative SNR versus FOV when b is varied with all the receivers (RX1~RX4) used (α=30° and γ=45°); **a.** FOV=70°, **b.** FOV=65°, **c.** FOV=60°, **d.** FOV=55°, **e.** FOV=50°, and **f** FOV=45°.

Then, we examined the influence of an FOV of a receiver on the SNR characteristics when all the receivers (RX1~RX4) are used in a diversity configuration with the MRC. Figures 11 show the results when an FOV is changed with the same parameters as in Figure 9(b) (α=30°, -90°≤β≤0°, and γ=45°) and the results are shown for an FOV of 70°, 65°, 60°, 55°, 50°, and 45°. From these results, we can see that the SNR characteristics are almost stable if an FOV is larger than 60°. However, for an FOV smaller than 55°, the minimum SNR characteristics is degraded for a certain value of β, which means that an optical receiver with more dynamic range will be required. Then, similar simulation has been carried out for the case of Figure 9 (a) (0°≤α≤90°, β=-30°, and γ=45°) and the results are shown in Figs. 12. We can see aforementioned tendency also in Figures 12.

From the discussion above, we have found that semi-angle of half illuminance of an LED should be about 55° for the best SNR. We have also made clear that an FOV smaller than 55° affects the diversity receiver performance.

Corresponding Author E-mail: sryu@meiji.ac.jp

Acta Materialia Turcica

Volume 4, June 2020, Pages 1-8

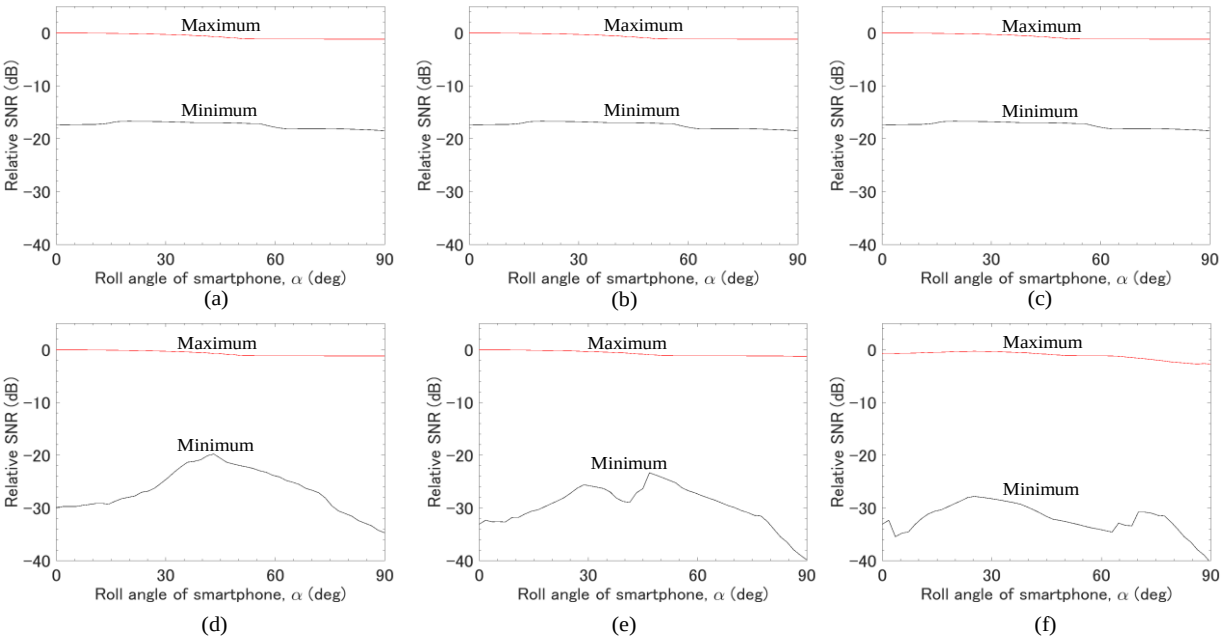

Figure 12. Relative SNR versus FOV when a is varied with all the receivers (RX1~RX4) used (α=-30° and γ=45°); **a.** FOV=70°, **b.** FOV=65°, **c.** FOV=60°, **d.** FOV=55°, **e.** FOV=50°, and **f.** FOV=45°.

6. CONCLUSIONS

Computer simulation has made it clear that four-receiver configuration proposed in the paper is effective for the OWC systems for smartphones under realistic usage conditions. It has also been made clear that there is an optimum value for a semi-angle at half illuminance of an LED, and it turned out to be about 55°. We have also pointed out that for an angle diversity receiver configuration proposed in this paper an FOV of each receiver should be larger than 60° to achieve stable receiver performance. If such a large FOV is difficult to achieve, we should consider the other receiver configuration to achieve narrower angle spacing of the adjacent receivers.

7. REFERENCES

[1] F. R. Gfeller and U. Bapst, Wireless in-house data communication via diffuse infrared radiation, Proc. IEEE 67 (1979) 1474-1486.

[2] J. M. Kahn and J. R. Barry, Wireless infrared communications, Proc. IEEE 85 (1997) 265-298.

[3] D. O'Brien, et al., High-speed optical wireless demonstrators: conclusions and future directions, IEEE Jour. Lightwave Technol. 30 (2012) 2181-2187.

[4] J. B. Carruthers and J. M. Kahn, Angle diversity for nondirected wireless infrared communication, IEEE Trans. Comm. 48 (2000) 960-969.

[5] Z. Chen, N. Serafimovski, and H. Haas, Angle diversity for an indoor cellular visible light communication system, Proc. IEEE Veh. Technol. Conf. (2014) 1–5, Seoul, South Korea.

[6] D. G. Brennan, Linear diversity combining techniques, Proc. IRE 47 (1959) 1075-1102.

Corresponding Author E-mail: sryu@meiji.ac.jp